Mean-Square Optical Anisotropy of Poly(*n*-hexyl isocyanate) in Dilute Solution

Masayuki Nakatsuji, Youichi Ogata, Masashi Osa, Takenao Yoshizaki, and Hiromi Yamakawa*

Department of Polymer Chemistry, Kyoto University, Kyoto 606-8501, Japan

Received June 26, 2001; Revised Manuscript Received September 14, 2001

ABSTRACT: The mean-square optical anisotropy $\langle\Gamma^2\rangle$ was determined from anisotropic light scattering measurements for nine samples of poly(*n*-hexyl isocyanate) (PHIC), a typical semiflexible polymer, in the range of weight-average molecular weight from 1.65×10^4 to 1.04×10^5 in *n*-hexane at 25.0 °C. It was found that the behavior of the ratio $\langle\Gamma^2\rangle/x_w$ as a function of the weight-average degree of polymerization x_w may be satisfactorily explained by the corresponding theory on the basis of the Kratky−Porod wormlike chain model with the respective values 840 Å and 71.5 $Å^{-1}$ of the basic model parameters, i.e., the static stiffness parameter λ^{-1} and the shift factor M_L, and also with the assigned value 1.1_2 $Å^2$ of the difference $\Delta\alpha$ between the polarizabilities, per unit contour length, parallel and perpendicular to the chain contour. The above value of $\Delta\alpha$ is appreciably larger than its value 0.5_3 $Å^2$ estimated from the bond polarizabilities on the basis of the chemical structure of PHIC, indicating that there exists definitely some additional scattered intensity arising from the effect of collision-induced polarizabilities. However, this does not affect the dependence itself of $\langle\Gamma^2\rangle/x_w$ on x_w. From a comparison of the present results for PHIC with previous ones for typical flexible polymers, it is seen that the difference in the behavior of $\langle\Gamma^2\rangle/x_w$ between them arises from that in chain stiffness.

Introduction

The mean-square optical anisotropy $\langle\Gamma^2\rangle$ as well as the mean-square radius of gyration $\langle S^2\rangle$ as a function of the degree of polymerization x may provide useful information about polymer chain stiffness and local chain conformations.[1] We have already carried out anisotropic light scattering (LS) measurements to determine $\langle\Gamma^2\rangle$ for atactic polystyrene (a-PS),[1,2] atactic poly(methyl methacrylate) (a-PMMA),[1,3] and isotactic (i-) PMMA[1,4] and shown that the data obtained for each polymer may be well explained by the corresponding theory on the basis of the helical wormlike (HW) chain model[1] with the use of the values of the model parameters consistent with those determined from $\langle S^2\rangle$ along with those of the local polarizability tensor reasonably assigned. All our studies made so far are restricted to typical flexible polymers, so that it is desirable to obtain data for $\langle\Gamma^2\rangle$ for typical semiflexible polymers and then to compare them with the theory and also with the data for the above flexible polymers.

Although there have been a number of experimental studies of the optical anisotropy of semiflexible polymers in dilute solution,[5] none of them have dealt with poly(*n*-hexyl isocyanate) (PHIC), a typical example of semiflexible polymers whose dilute solution properties have been almost thoroughly investigated. This may probably be due to the fact that its optical anisotropy is not sufficiently large to determine $\langle\Gamma^2\rangle$ precisely, as seen from the data obtained by Jinbo et al.[6] in moderately concentrated solution. In this work, we tackle the problem to determine $\langle\Gamma^2\rangle$ for PHIC in dilute solution (in *n*-hexane at 25.0 °C) despite the rather difficult experimental condition in order to investigate its dependence on x.

Now it is well-known that the PHIC chain in *n*-hexane preserves the Schmueli−Traub−Rosenheck[7] 8_3 helices[8−10] and that the equilibrium conformational behavior of its helix axis may be well represented by the Kratky−Porod (KP) wormlike chain.[1,11] All the local physical quantities such as the local polarizability tensor affixed to the chain may therefore be considered to be cylindrically symmetric around the axis. Then the parameters necessary for the theoretical calculation of $\langle\Gamma^2\rangle$ are the difference $\Delta\alpha$ between the polarizabilities parallel and perpendicular to the axis and the two basic KP model parameters: the static stiffness parameter λ^{-1} and the shift factor M_L as defined as the molecular weight per unit contour (or helix axis in this case) length. While the values of these KP model parameters have already been determined rather unambiguously,[9] the parameter $\Delta\alpha$ remains unknown. In this paper, we regard $\Delta\alpha$ as an adjustable parameter to determine so that the experimental and theoretical values of $\langle\Gamma^2\rangle$ are in good agreement with each other and then compare the determined value of $\Delta\alpha$ with that estimated from the bond polarizabilities on the basis of the chemical structure of PHIC.

For the present anisotropic LS measurements, we adopt an improved data acquisition procedure different from that used for our usual isotropic LS measurements in order to increase reliability.

Experimental Section

Materials. As in the previous study of the dynamic structure factor of PHIC,[12] the original PHIC samples were prepared following the procedure of Aharoni.[13] The polymerization was carried out in a toluene/*N*,*N*-dimethylformamide (1:1) mixture at −78 °C with sodium cyanide as an initiator and methanol as a terminator. All the test samples except the one with the highest molecular weight are fractions separated from the original samples by fractional precipitation using benzene as a solvent and methanol as a precipitant. The highest molecular weight sample PHIC10 is the same as that used in the previous study.[12]

The solvent *n*-hexane used for all measurements was purified according to a standard procedure prior to use.

10.1021/ma011103k CCC: $20.00
Published on Web 10/26/2001

Light Scattering. LS measurements were carried out to determine the weight-average molecular weight M_w and $\langle\Gamma^2\rangle$ for all the samples and also $\langle S^2\rangle$ for the samples with $M_w \gtrsim 4 \times 10^4$ in *n*-hexane at 25.0 °C. A Fica 50 light-scattering photometer was used for all the measurements with vertically (v) polarized incident light of wavelength $\lambda_0 = 436$ nm.

Before proceeding to give a description of the experimental procedure, it is pertinent to refer here to modifications made in our photometer. Since it had been having trouble with its circuits, we replaced all of them except the chopper one by a couple of programmable digital voltmeters (Yokogawa model 7551) controlled by a personal computer. In the photometer so modified, the outputs from the chopper circuit, i.e., the incident and scattered light intensities converted into voltage, were independently measured by the voltmeters, each with an integration time of 100 ms. The two kinds of voltage were alternately recorded on the computer at intervals of ca. 150 ms, and then each scattered intensity was divided by a mean of its preceding and following incident light intensities to determine the corrected scattered intensity, which does not suffer from fluctuations in the incident light intensity (brightness of a mercury lamp). For the unpolarized (Uv) component of the scattered intensity, 20 successive corrected intensities were averaged to obtain a final observed value, as done so far. For the depolarized (Hv) component, which is very weak compared to the Uv one, more than 60 successive reduced intensities were accumulated to determine the average value in order to reduce experimental error. In addition to the above modifications of the circuits, a pair of pieces of Polaroid with an extinction ratio of ca. 10^{-2} originally used as a polarizer and an analyzer were replaced by Gran-Thompson prisms with an extinction ratio smaller than 10^{-5}, as previously[14] mentioned.

For a calibration of the apparatus, the Uv and Hv components of the intensity of light scattered from pure benzene were measured at 25.0 °C at a scattering angle θ of 90° without and with the analyzer, respectively. The apparatus constants in the cases of the Uv and Hv measurements were estimated from the experimental values of the respective intensities so determined and also from the values of the Uv and Hv components of the reduced intensity absolutely determined. The latter absolute values were calculated from the literature value[15] 46.5×10^{-6} cm^{-1} of the Rayleigh ratio $R_{Uu}(90°)$ and the experimental value 0.41 ± 0.01 of the depolarization ratio ρ_u of pure benzene at 25.0 °C.

Thus, the Uv and Hv components of the scattered intensity were measured for all the samples at four or five different concentrations and at θ ranging from 30° to 142.5° in *n*-hexane at 25.0 °C. We used the literature value[9] 0.134 cm^3/g of the refractive index increment for PHIC in *n*-hexane at 25.0 °C along with the value 1.380 of the refractive index n_0 of *n*-hexane at 25.0 °C, both at $\lambda_0 = 436$ nm.

The most concentrated solution of each sample was prepared gravimetrically and made homogeneous by continuous stirring at ca. 50 °C for 1 or 2 days. It was optically purified by filtration through a Teflon membrane of pore size 0.45 or 1.0 μm. The solutions of lower concentrations were obtained by successive dilution, adding the solvent optically purified by filtration through a Teflon membrane of pore size 0.1 μm. The weight concentrations of the test solutions were converted to the polymer mass concentrations *c* by the use of the densities of the solutions.

Results

Characterization. According to the theories on the basis of the Gaussian chain model[16] and also the KP[17] and HW[18] chain models, the excess unpolarized (Uv) and depolarized (Hv) components, ΔR_{Uv} and ΔR_{Hv}, of the reduced scattered intensity determined from LS measurements with vertically polarized incident light may be related to M_w in the limit of $c \to 0$ and $\theta \to 0$ by the equations

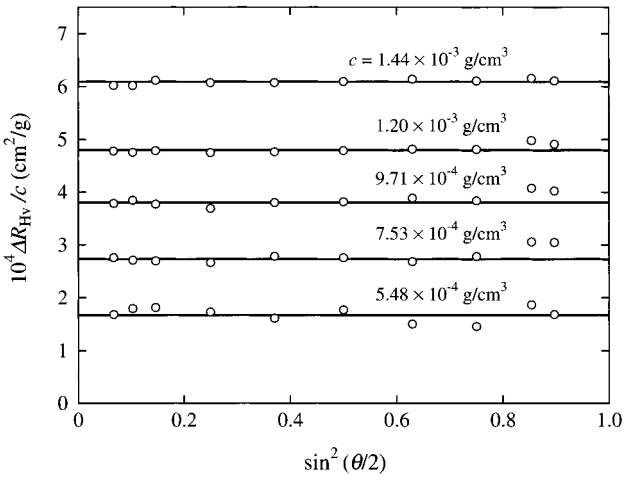

Figure 1. Plots of $\Delta R_{Hv}/c$ against $\sin^2(\theta/2)$ for the PHIC sample PHIC5 in *n*-hexane at 25.0 °C for the indicated value of *c*. The data points at $c = 7.53 \times 10^{-4}$, 9.71×10^{-4}, 1.20×10^{-3}, and 1.44×10^{-3} g/cm^3 are shifted upward by 1×10^{-4}, 2×10^{-4}, 3×10^{-4}, and 4×10^{-4} cm^2/g, respectively.

$$\lim_{c,\theta\to 0} \frac{\Delta R_{Uv}}{2Kc} = (1 + 7\delta)M_w \tag{1}$$

$$\lim_{c,\theta\to 0} \frac{\Delta R_{Hv}}{2Kc} = 3\delta M_w \tag{2}$$

where *K* is the optical constant and δ is a parameter representing the anisotropy of the local polarizability tensor affixed to the statistical segment or the chain contour. Then the values of M_w and δ for a given sample may be simultaneously determined from the experimental values of $(\Delta R_{Uv}/2Kc)_{c=0,\theta=0}$ and $(\Delta R_{Hv}/2Kc)_{c=0,\theta=0}$.

The value of $(\Delta R_{Uv}/2Kc)_{c=0,\theta=0}$ may readily be determined from the Berry square-root plot.[19] However, the determination of $(\Delta R_{Hv}/2Kc)_{c=0,\theta=0}$ requires some comments. The theoretical ΔR_{Hv} is independent of θ for the Gaussian chain model[16] but in general depends on θ for the KP[17] and HW[18] chain models. Strictly, therefore, the values of $\Delta R_{Hv}/2Kc$ determined at finite θ (and also at very low but finite *c*) should be extrapolated to $\theta = 0$ by the use of an appropriate theoretical curve, for instance, the KP theory values at infinite dilution. In fact, however, for the KP chains corresponding to the present PHIC samples the variations of the theoretical values of ΔR_{Hv} around the respective mean values over the range of θ measured are within ±3%. Thus, we simply adopted as the experimental value of $(\Delta R_{Hv}/2Kc)_{\theta=0}$ (at finite *c*) a mean of values of $\Delta R_{Hv}/2Kc$ determined at different θ. A possible error arising from this rather simplified procedure may be considered not to exceed an experimental error in $\Delta R_{Hv}/2Kc$, which is appreciably larger than that in $\Delta R_{Uv}/2Kc$.

As an example, plots of $\Delta R_{Hv}/c$ against $\sin^2(\theta/2)$ for the sample PHIC5 in *n*-hexane at 25.0 °C are shown in Figure 1 for the indicated values of *c*. At any *c*, an appreciable dependence of $\Delta R_{Hv}/c$ on $\sin^2(\theta/2)$ cannot be observed in the range of θ studied, being buried in the scatter of data points. The horizontal straight line associated with the data points at each *c* represents the mean value. The standard deviations of the experimental values shown in the figure are 2% at the highest concentration and 7% at the lowest concentration. The values of $(\Delta R_{Hv}/c)_{\theta=0}$ so determined are plotted against *c* in Figure 2 for all the samples in *n*-hexane at 25.0 °C. The vertical line segments attached to the data points

Table 1. Results of LS Measurements for Poly(*n*-hexyl isocyanate) in *n*-Hexane at 25.0 °C

sample	$10^{-4}M_w$	x_w	$10^3\delta$	$10^{-4}\langle S^2\rangle$, Å^2	$10^{-4}\langle\Gamma^2\rangle$, Å^6	$10^{-2}\langle\Gamma^2\rangle/x_w$, Å^6	M_w/M_n[b]
PHIC1	1.65	130	2.2_7		3.9_4	3.0_3	1.10
PHIC2a	2.18	172	1.9_7		5.9_5	3.4_6	1.10
PHIC2b	2.66	209	1.8_1		8.1_7	3.9_1	1.07
PHIC3	2.90	228	1.8_5		9.8_9	4.3_4	1.10
PHIC4	4.71	371	1.2_5	3.1_8	$17._7$	4.7_7	1.04
PHIC5	5.71	450	1.1_3	4.3_6	$23._4$	5.2_0	1.05
PHIC7	7.67	604	0.90_8	6.8_1	$34._0$	5.6_3	1.06
PHIC8	8.42	663	0.85_9	7.7_2	$38._8$	5.8_5	1.03
PHIC10	10.4[a]	819	0.82_4	$10._2$[a]	$48._2$	5.8_9	1.03

[a] Reproduced from ref 12. [b] Determined by analytical GPC.

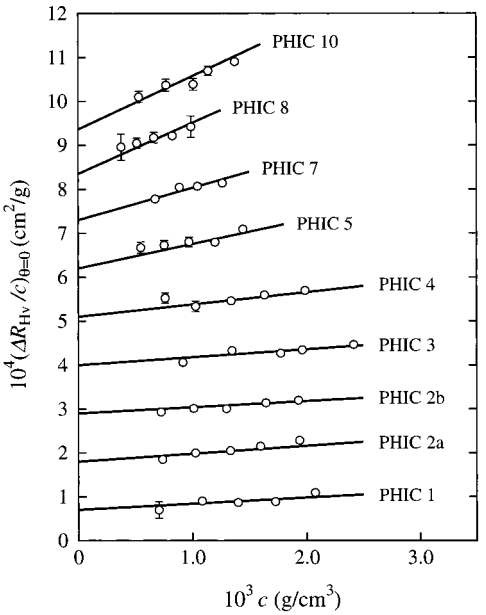

Figure 2. Plots of $(\Delta R_{Hv}/c)_{\theta=0}$ against c for the PHIC samples indicated in *n*-hexane at 25.0 °C. The data points for the samples PHIC2a through PHIC10 are shifted upward by 1×10^{-4}, 2×10^{-4}, 3×10^{-4}, 4×10^{-4}, 5×10^{-4}, 6×10^{-4}, 7×10^{-4}, and 8×10^{-4} cm^2/g, respectively. The vertical line segments attached to the data points indicate the error bounds.

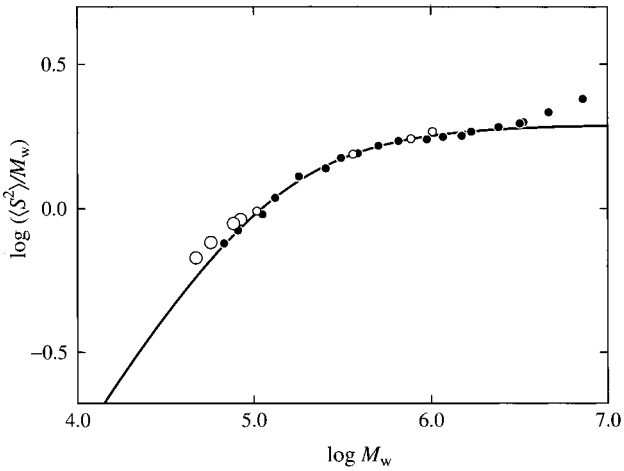

Figure 3. Double-logarithmic plots of $\langle S^2\rangle/M_w$ against M_w for PHIC in *n*-hexane at 25.0 °C: (◯) present data; (○) previous data;[12] (●) data by Murakami et al.[9] The solid curve represents the KP theory values calculated from eq 3 with eq 4 with $\lambda^{-1} = 840$ Å and $M_L = 71.5$ Å^{-1}.

indicate the error bounds estimated from the standard deviations. The data points for each sample were extrapolated to infinite dilution by the straight line shown in the figure in order to determine $(\Delta R_{Hv}/c)_{c=0,\theta=0}$.

In the fourth column of Table 1 are given the values of δ for all the samples in *n*-hexane at 25.0 °C calculated from eqs 1 and 2 with the values of $(\Delta R_{Uv}/2Kc)_{c=0,\theta=0}$ and $(\Delta R_{Hv}/2Kc)_{c=0,\theta=0}$ determined above. It is seen from these values that the values of the ratio $(\Delta R_{Hv}/\Delta R_{Uv})_{c=0,\theta=0} \simeq 3\delta$ are even smaller than 10^{-2}. It is then reconfirmed that the optical anisotropy of PHIC is very small. For this polymer, therefore, no corrections of the optical anisotropy to M_w and $\langle S^2\rangle$ have been made, and M_w and $\langle S^2\rangle$ have been determined by the use of the Berry plot of $(2Kc/\Delta R_{Uv})^{1/2}$ against c and/or $\sin^2(\theta/2)$.[6,9,12] As is well-known, the molecular weight determined from this plot is not M_w but the apparent weight-average molecular weight $M_{w,ap} = M_w(1 + 7\delta)$ if δ cannot be neglected (see eq 1). We made corrections to M_w for those samples whose 7δ are larger than 10^{-2}, i.e., for the samples PHIC1 through PHIC3. We note that the difference between M_w and $M_{w,ap}$ does not exceed 1.6%. In the determination of M_w for the samples PHIC4 through PHIC10, we neglected the term 7δ in eq 1. In the second and third columns of Table 1 are given the values of M_w so determined and also those of the weight-average degree of polymerization x_w calculated from the M_w values with the value 127 of the molecular weight of the repeat unit.

In the fifth column of Table 1 are given the values of $\langle S^2\rangle$ determined for the samples PHIC4 through PHIC10 in *n*-hexane at 25.0 °C without consideration of the effect of the optical anisotropy. This effect on $\langle S^2\rangle$ for these samples may be considered to be negligibly small as in the case of M_w. For the samples PHIC1 through PHIC3, $\langle S^2\rangle$ could not be accurately determined. The values of the ratio of M_w to the number-average molecular weight M_n determined by analytical GPC for all the samples are also given in the last column of Table 1.

Figure 3 shows double-logarithmic plots of $\langle S^2\rangle/M_w$ against M_w for PHIC in *n*-hexane at 25.0 °C. The large unfilled circles represent the experimental values obtained in the present work, and the three small ones represent those previously obtained in the study of the dynamic structure factor of PHIC in the same solvent condition.[12] Of the latter three samples, the one with the lowest M_w (PHIC10) was also used in the present study of $\langle\Gamma^2\rangle$. The filled circles represent the experimental values obtained by Murakami et al.[9] The solid curve represents the KP theory values calculated from[1,20]

$$\langle S^2\rangle = \frac{L}{6\lambda} - \frac{1}{4\lambda^2} + \frac{1}{4\lambda^3 L} - \frac{1}{8\lambda^4 L^2}(1 - e^{-2\lambda L}) \quad (3)$$

where L is the total contour length and is related to the molecular weight M by

$$L = M/M_L \quad (4)$$

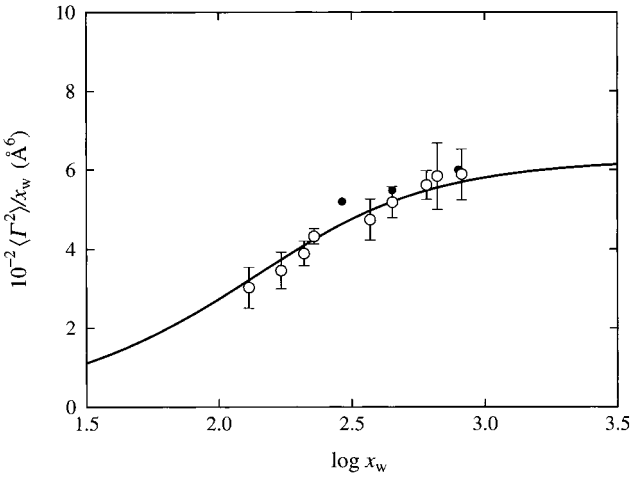

Figure 4. Plots of $\langle\Gamma^2\rangle/x_w$ against log x_w for PHIC: (○) present data in *n*-hexane at 25.0 °C; (●) data by Jinbo et al.[6] in toluene at 25.0 °C. The vertical line segments attached to the present data points indicate the error bounds. The solid curve represents the best-fit KP theory values calculated from eq 6 with eq 8 with $M_0 = 127$, $\Delta\alpha = 1.1_2$ Å^2, $\lambda^{-1} = 840$ Å, and $M_L = 71.5$ Å^{-1}.

with $\lambda^{-1} = 840$ Å and $M_L = 71.5$ Å^{-1}.[9] As seen from the figure, our present and previous[12] data are consistent with those by Murakami et al.[9] within experimental error, and the data of the two groups are rather well fitted by the theoretical curve in the range of $M_w \lesssim 3 \times 10^6$. Note that the excluded-volume effect becomes appreciably large for $M_w \gtrsim 3 \times 10^6$.

Mean-Square Optical Anisotropy. If the effect of the internal electric field is taken into account by the use of the Lorentz−Lorenz equation and if the effect of collision-induced polarizabilities[2,14] is ignored, the mean-square optical anisotropy $\langle\Gamma^2\rangle$ may be calculated from

$$\langle\Gamma^2\rangle = \frac{15\lambda_0{}^4}{16\pi^4}\frac{M_w}{N_A}\left(\frac{3}{n_0{}^2+2}\right)^2\left(\frac{\Delta R_{Hv}}{c}\right)_{c=0,\theta=0} \quad (5)$$

with the experimental value of $(\Delta R_{Hv}/c)_{c=0,\theta=0}$ determined above, where λ_0 is the wavelength of the incident light in a vacuum and is equal to 436 nm, N_A is the Avogadro constant, and n_0 is the refractive index of the solvent. Equation 5 requires some comments. There are some objections to the use of the above second-power-type correction (Lorentz−Lorenz equation). However, we already discussed this point thoroughly in the previous study of $\langle\Gamma^2\rangle$ of a-PMMA[3] and thus have adopted above the same correction as that previously[2−4] used. Note that this adoption never affects the dependence itself of $\langle\Gamma^2\rangle$ on x_w but alters only the assigned value of $\Delta\alpha$. The neglect of collision-induced polarizabilities has a similar effect, and the effect is discussed in the next section. Thus, the use of eq 5 does not injure a comparison of the present results with previous ones.

The values of $\langle\Gamma^2\rangle$ calculated from eq 5 with the values of $(\Delta R_{Hv}/c)_{c=0,\theta=0}$ determined in the last subsection are given in the sixth column of Table 1. There are also given the values of $\langle\Gamma^2\rangle/x_w$ in the seventh column. Figure 4 shows plots of $\langle\Gamma^2\rangle/x_w$ against the logarithm of x_w for PHIC in *n*-hexane at 25.0 °C. The unfilled circles represent the present experimental values, where the vertical line segments attached to the data points indicate the error bounds. The filled circles represent the values estimated by extrapolation to infinite dilution from the results by Jinbo et al.[6] for moderately concentrated solutions of PHIC in toluene at 25.0 °C. We note that $\lambda^{-1} = 740$ Å and $M_L = 74.0$ Å^{-1} for PHIC in toluene at 25.0 °C,[21] so that the conformations of the PHIC chain in toluene and in *n*-hexane at 25.0 °C may be considered not to be very different. The present data are consistent with those by Jinbo et al.[6] within experimental error. It is seen from the figure that $\langle\Gamma^2\rangle/x_w$ increases monotonically with increasing x_w and then approaches its asymptotic value. In the figure, the solid curve represents the KP theoretical values, which are mentioned in the next section.

Discussion

Comparison with Theory. The mean-square optical anisotropy $\langle\Gamma^2\rangle$ for the KP chain is given by[17,18,22]

$$\frac{\langle\Gamma^2\rangle}{x} = \frac{\lambda^{-1}M_0}{3M_L}(\Delta\alpha)^2\left[1 - \frac{1}{6\lambda L}(1 - e^{-6\lambda L})\right] \quad (6)$$

where $\Delta\alpha$ is the difference between the polarizabilities, per unit contour length, parallel and perpendicular to the contour, which we denote by $\alpha_\parallel$ and $\alpha_\perp$, respectively, i.e.

$$\Delta\alpha = |\alpha_\parallel - \alpha_\perp| \quad (7)$$

and L is related to x by

$$L = xM_0/M_L \quad (8)$$

with M_0 the molecular weight of the repeat unit.

In Figure 4, the solid curve represents the best-fit KP theory values calculated from eq 6 with eq 8 with $M_0 = 127$, $\Delta\alpha = 1.1_2$ Å,[2] and the basic model parameter values, $\lambda^{-1} = 840$ Å and $M_L = 71.5$ Å^{-1}.[9] As mentioned in the Introduction, $\Delta\alpha$ has been treated as an adjustable parameter and determined to give the above best-fit theoretical curve. It is seen that the theory may rather well explain the dependence of $\langle\Gamma^2\rangle/x_w$ on x_w.

Local Polarizability Tensor. Now we estimate the value of $\Delta\alpha$ for PHIC by the use of literature values of the bond polarizability tensors. For this purpose, in parts a and b of Figure 5 are shown side and bottom views, respectively, of the skeleton of one turn of the (rigid) helix of PHIC with a localized Cartesian coordinate system (ξ, η, ζ) affixed to it. Here, we have assumed that the two kinds of rotation angles around the C−N bonds in the main chain take the values given by Troxell and Scheraga[8] for poly(methyl isocyanate) and also that each *n*-hexyl group takes the all-*trans* conformation and is attached to the N atom with its axis of symmetry making a right angle with the helix axis (with the minimum energy) for simplicity. The same bottom view as that in Figure 5b is shown in Figure 5c, where all atoms are depicted by the spheres having the van der Waals radii and the circle of diameter 16 Å determined from the intrinsic viscosity[9] $[\eta]$ is also drawn. It is seen from Figure 5c that the above two assumptions are not so unrealistic.

In the evaluation of $\Delta\alpha$, we only need the bond polarizability tensors averaged over the rotation around the ζ axis, each of the resultant averaged tensors being cylindrically symmetric around the ζ axis, i.e., of the form of a 3 × 3 tensor with the $\xi\xi$ and $\eta\eta$ components being identical with each other. The absolute values of the angles between the ζ axis and the bonds necessary

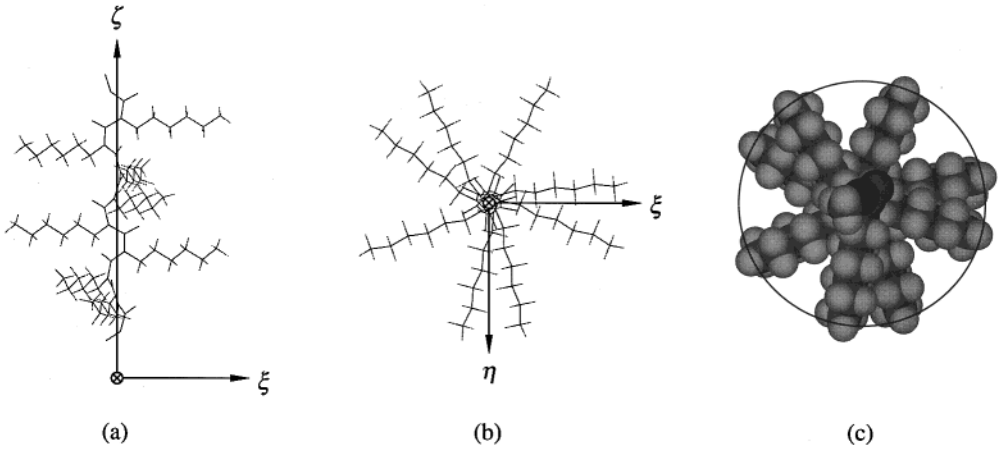

Figure 5. Schematic drawing of the helix of PHIC with a localized Cartesian coordinate system affixed to it: (a) side view of its skeleton; (b) bottom view of its skeleton; (c) bottom view, where all atoms are depicted by the spheres (see the text). The circle in (c) has the diameter of 16 Å determined from $[\eta]$.[9]

for the evaluation of the $\zeta\zeta$ ($\|$) and $\xi\xi$ (or $\eta\eta$) ($\perp$) components of the averaged tensors have been given by Troxell and Scheraga.[8] We have used the literature values of the bond polarizability tensors for the C−H,[23] C−C,[23] C−N,[24] and C−O[23] bonds, which are summarized in ref 25. As for the C═O bond, we have estimated its polarizability tensor by the use of the literature value for methyl acetate[25,26] along with the above values for C−H, C−C, and C−O bonds, assuming the additivity of bond polarizabilities. With the correction made by multiplying all the bond polarizability tensors by the common factor $\sqrt{1.9_4}$,[3] $\Delta\alpha$ is then estimated to be 0.5_3 Å^2, which is appreciably smaller than the value 1.1_2 Å^2 determined above.

The above difference between the experimental and calculated values of $\Delta\alpha$ indicates that there exists definitely some additional scattered intensity arising from the effect of collision-induced polarizabilities, although the latter value of $\Delta\alpha$ may probably be somewhat underestimated. However, this does not affect the dependence itself of $\langle\Gamma^2\rangle$ on x_w, as already mentioned in the Results section.

Comparison with Other Polymers. For comparison, values of $\langle\Gamma^2\rangle/x_w$ for other polymers along with those for PHIC are double-logarithmically plotted against x_w in Figure 6. The unfilled and filled circles represent the present experimental values obtained for PHIC in *n*-hexane at 25.0 °C and the literature ones[6] for PHIC in toluene at 25.0 °C, respectively, both already shown in Figure 4. The unfilled squares, triangles, and inverted triangles represent the values previously obtained for a-PS in cyclohexane at 34.5 °C (Θ),[2,3] a-PMMA in acetonitrile at 44.0 °C (Θ),[3] and i-PMMA in acetonitrile at 28.0 °C (Θ),[4] respectively. As an example of semiflexible polymers other than PHIC, there are also plotted the literature values obtained by Sakurai et al.[27] for poly(terephthalamide-*p*-benzohydrazide) (PPAH) in dimethyl sulfoxide at 25.0 °C (filled squares). The solid and dashed curves associated with the data points represent the KP and HW theory values for the semiflexible polymers PHIC and PPAH and for the flexible polymers a-PS, a-PMMA, and i-PMMA. The KP theory values for PPAH have been calculated from eq 6 with eq 8 with $M_0 = 281$, $\Delta\alpha = 2.2$ Å^2, $\lambda^{-1} = 224$ Å, and $M_L = 18.5$ Å^{-1}, where the value of $\Delta\alpha$ has been estimated from the value 2.1 of the parameter ϵ used by Sakurai et al. The HW theory values have been reproduced from the previous papers.[3,4]

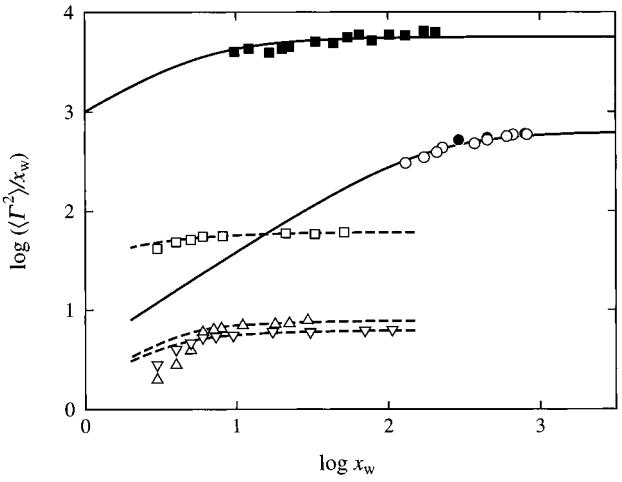

Figure 6. Double-logarithmic plots of $\langle\Gamma^2\rangle/x_w$ against x_w: (○) present data for PHIC in *n*-hexane at 25.0 °C; (●) data by Jinbo et al. for PHIC in toluene at 25.0 °C;[6] (□) previous data for a-PS in cyclohexane at 34.5 °C (Θ);[2,3] (△) previous data for a-PMMA in acetonitrile at 44.0 °C (Θ);[3] (▽) previous data for i-PMMA in acetonitrile at 28.0 °C (Θ);[4] (■) data by Sakurai et al. for PPAH in dimethyl sulfoxide at 25.0 °C.[27] The solid and dashed curves represent the KP and HW theory values, respectively (see text).

The asymptotic value of $\langle\Gamma^2\rangle/x_w$ in the limit of $x_w \to \infty$ for PHIC is very large compared to those for the three flexible polymers, although $\Delta\alpha$ of PHIC is of the same order of magnitude as the polarizability tensors assigned to the three flexible chains. Furthermore, the value of x_w where $\langle\Gamma^2\rangle/x_w$ reaches its asymptotic value is also remarkably larger for PHIC than for the flexible polymers. This is, of course, due to the fact that λ^{-1} of PHIC is very large compared to those of typical flexible polymers. PPAH has the largest asymptotic value of all the polymers shown in Figure 6. This is because its $\Delta\alpha$ is appreciably larger than those of the others.

Finally, we must note that the experimental errors in the values of $\langle\Gamma^2\rangle$ previously determined for the flexible polymers may be considered to be smaller than those in the present values for PHIC despite the fact that $\langle\Gamma^2\rangle$ is much smaller for the former than for the latter. The reason for this is that the range of *c* adopted for the present measurements is far lower than those for the flexible polymers, which were from ca. 0.1 to ca. 0.3 g/cm^3.

Conclusion

We could determine the mean-square optical anisotropy $\langle\Gamma^2\rangle$ for PHIC, whose optical anisotropy is very small, within permissible experimental error. It was then found that the dependence of $\langle\Gamma^2\rangle/x_w$ on x_w may be satisfactorily explained by the corresponding theory on the basis of the KP chain model. The assigned value of $\Delta\alpha$ is appreciably larger than its value estimated from the bond polarizabilities, indicating that there exists definitely some additional scattered intensity arising from the effect of collision-induced polarizabilities. However, this does not affect the dependence itself of $\langle\Gamma^2\rangle/x_w$ on x_w. From a comparison of the present results for PHIC with the previous ones for the typical flexible polymers, it is seen that the difference in the behavior of $\langle\Gamma^2\rangle$ between them arises from that in chain stiffness as in the cases of $\langle S^2\rangle$ and also the transport coefficients (intrinsic viscosity and translational diffusion coefficient).[1]

References and Notes

(1) Yamakawa, H. *Helical Wormlike Chains in Polymer Solutions*; Springer: Berlin, 1997.
(2) Konishi, T.; Yoshizaki, T.; Shimada, J.; Yamakawa, H. *Macromolecules* **1989**, *22*, 1921.
(3) Takaeda, Y.; Yoshizaki, T.; Yamakawa, H. *Macromolecules* **1993**, *26*, 3742.
(4) Takaeda,Y.; Yoshizaki, T.; Yamakawa, H. *Macromolecules* **1995**, *28*, 4167.
(5) Norisuye,T. *Prog. Polym. Sci.* **1993**, *18*, 543 and papers cited therein.
(6) Jinbo, Y.; Varichon, L.; Sato, T.; Teramoto, A. *J. Chem. Phys.* **1998**, *109*, 8081.
(7) Schmueli, U.; Traub, W.; Rosenheck, K. *J. Polym. Sci., Part A-2* **1969**, *7*, 515.
(8) Troxell, T. C.; Scheraga, H. A. *Macromolecules* **1971**, *4*, 528.
(9) Murakami, H.; Norisuye, T.; Fujita, H. *Macromolecules* **1980**, *13*, 345.
(10) (a) Lifson, S.; Felder, C. E.; Green, M. M. *Macromolecules* **1992**, *25*, 4142. (b) Green, M. M.; Peterson, N. C.; Sato, T.; Teramoto, A.; Cook, R.; Lifson, S. *Science* **1995**, *268*, 1860.
(11) Kratky, O.; Porod, G. *Recl. Trav. Chim.* **1949**, *68*, 1106.
(12) Yoshida, N.; Yoshizaki, T.; Yamakawa, H. *Macromolecules* **2000**, *33*, 3254.
(13) Aharoni, S. M. *Macromolecules* **1979**, *13*, 409.
(14) Yoshizaki, T.; Yamakawa, H. *Chem. Lett.* **1987**, 2351.
(15) Deželić, Gj.; Vavra, J. *Croat. Chem. Acta* **1966**, *38*, 35.
(16) (a) Utiyama, H.; Kurata, M. *Bull. Inst. Chem. Res. Kyoto Univ.* **1964**, *42*, 128. (b) Utiyama, H. *J. Phys. Chem.* **1965**, *69*, 4138.
(17) Nagai, K. *Polym. J.* **1972**, *3*, 67.
(18) Yamakawa, H.; Fujii, M.; Shimada, J. *J. Chem. Phys.* **1979**, *71*, 1611.
(19) Berry, G. C. *J. Chem. Phys.* **1966**, *44*, 4550.
(20) Benoit, H.; Doty, P. *J. Phys. Chem.* **1953**, *57*, 958.
(21) Itou, T.; Chikiri, H.; Teramoto, A.; Aharoni, S. M. *Polym. J.* **1988**, *20*, 143.
(22) Arpin, A.; Strazielle, C.; Weill, G.; Benoit. H. *Polymer* **1977**, *18*, 262.
(23) Patterson, G. D.; Flory, P. J. *J. Chem. Soc., Faraday Trans.* **1972**, *68*, 1098; **1972**, *68*, 1111.
(24) Le Fevre, C. G.; Le Fevre, R. J. W. *Rev. Pure Appl. Chem.* **1955**, *5*, 261; **1970**, *20*, 57.
(25) Riande, E.; Saiz, E. *Dipole Moments and Birefringence of Polymers*; Prentice Hall: Englewood Cliffs, NJ, 1992.
(26) Flory, P. J.; Saiz, E.; Erman, B.; Irvine, P. A.; Hummel, J. P. *J. Phys. Chem.* **1981**, *85*, 3215.
(27) Sakurai, K.; Ochi, K.; Norisuye, T.; Fujita. H. *Polym. J.* **1984**, *16*, 559.

MA011103K